


Large Pore Size Nanoporous Materials from the Self-Assembly of Asymmetric Bottlebrush Block Copolymers

Justin Bolton,[†] Travis S. Bailey,[‡] and Javid Rzayev^{*,†}

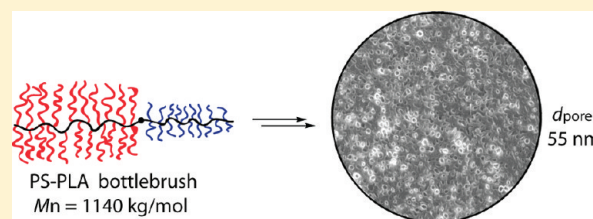
[†]Department of Chemistry, University at Buffalo, The State University of New York, Buffalo, New York 14260-3000, United States

[‡]Department of Chemical and Biological Engineering, Colorado State University, Fort Collins, Colorado 80523-1370, United States

 Supporting Information

ABSTRACT: Asymmetric polystyrene–polylactide (PS–PLA) bottlebrush block copolymers have been shown to self-assemble into a cylindrical morphology with large domain spacings. PLA cylinders can be selectively etched out of the shear-aligned polymer monoliths to generate nanoporous materials with an average cylindrical pore diameter of 55 nm. The remaining bottlebrush backbone provides a functional, hydrophilic coating inside the nanopores. This methodology significantly expands the range of pore sizes attainable in block copolymer based nanoporous materials.

KEYWORDS: Nanoporous materials, bottlebrush, block copolymers, self-assembly, polylactide



Melt-state self-assembly of block copolymers provides access to a variety of nanostructured morphologies.^{1,2} One of the burgeoning endeavors in this field is the fabrication of nanoporous materials by selective removal of one of the constituent blocks from a self-assembled block copolymer precursor.³ Such materials can provide superior selectivity and fluxes compared to the currently utilized phase-inversion and track-etch membranes and bear tremendous potential for an array of applications, such as filtration,^{4,5} selective crystallization,⁶ and templating.^{7,8} However, practical limitations of high molecular weight linear block copolymer self-assembly, namely, high entanglement densities and prohibitively slow ordering kinetics, restrict the size scale of attainable nanoporous materials producible on their basis. Typically, self-assembly of linear block copolymers provides well-ordered nanomaterials with domain spacings of 5–50 nm, which results in the largest realistically attainable pore sizes of about 35 nm.^{3,9} Since the above-mentioned applications rely on the availability of nanoporous materials with a wide range of finely tuned pore sizes, an ongoing challenge in this field is circumventing the limitations of linear block copolymer self-assembly and gaining access to nanoporous materials with larger pore sizes while maintaining comparable high porosity and pore size distributions. In this report, we demonstrate that asymmetric bottlebrush block copolymers with carefully tuned architectures can self-organize into cylindrical morphologies that serve as precursors for nanoporous materials with cylindrical pore diameters of >50 nm.

Bottlebrush copolymers, or molecular brushes, are a class of densely branched macromolecules with a comblike architecture.^{10,11} There is a growing interest in the self-assembly of these copolymers at different interfaces.^{12–15} Recent studies on bottlebrush block copolymer melt self-assembly by our group and

others^{16,17} have demonstrated that these macromolecules can organize into highly ordered microstructures despite their large size (>1 million g/mol). Lamellae morphologies were observed exclusively, with attained domain spacings of as large as 160 nm. Such a predilection toward the formation of flat interfaces can be attributed to the semirigid nature of molecular brushes. We previously reported that even bottlebrush block copolymers with a highly asymmetric composition ($f_A = 0.3$) form remarkably ordered lamellae microstructures if the brush length in two blocks is kept constant.¹⁷

The morphology attained by a diblock copolymer is dictated by relative sizes of its constituent blocks (in the high segregation limit).¹ In a traditional linear diblock copolymer, the composition can be varied by only one parameter—the length of polymer chains comprising the blocks. Polymer chain length, in turn, is directly correlated to the 3D size of the polymer molecule through a simple power law ($R_g \sim N^a$), where the exponent a is typically in the range of 0.5–0.6 for most flexible polymers existing as random coils. On the other hand, in a bottlebrush architecture, there are two distinct variables that control polymer composition, the length of the backbone and the length of the brush side chains. Changing these two parameters can provide the same average compositions but will result in a dramatically different polymer size and shape as a result of the two-dimensional nature of the bottlebrush molecular architecture. The two effects can be easily visualized if a bottlebrush molecule is approximated as a soft cylinder. Since the bottlebrush backbone is already highly extended, increasing its size leads to the formation

Received: October 25, 2010

Revised: December 23, 2010

Published: January 31, 2011

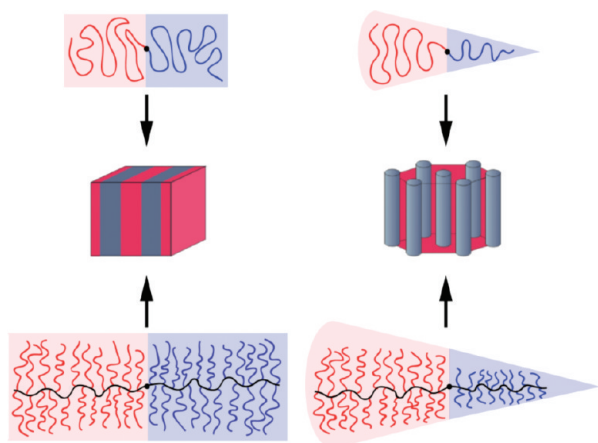
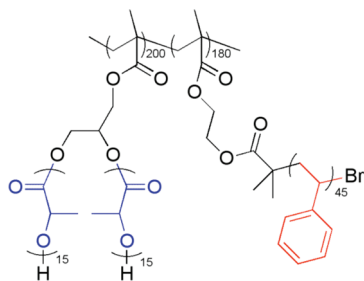


Figure 1. Control of the interfacial curvature during self-assembly of linear (top) and bottlebrush (bottom) block copolymers.

Scheme 1



of an elongated cylindrical molecule and does not have a significant effect on its cross-sectional area, the parameter most important for controlling molecular packing. On the other hand, increasing the size of side chain branches will dramatically change the cross-sectional area of the cylindrical bottlebrush macromolecule. Thus, highly asymmetric molecular objects can be prepared, where a bottlebrush block copolymer contains shorter branches on one side and longer branches on the other side. The overall asymmetric shape of such polymer molecules will be analogous to compositionally asymmetric linear diblock copolymers and thus should favor the formation of morphologies with curved interfaces (Figure 1).

Herein, we demonstrate that an asymmetric polystyrene–polylactide (PS–PLA) bottlebrush block copolymer with long PS branches and shorter PLA branches can attain a cylindrical morphology upon melt self-assembly. We show that the cylindrical morphology can be aligned, and PLA domains selectively etched out to provide nanoporous materials with previously unattainable pore sizes. This is the first report of the preparation of nonlamellae morphologies from the bottlebrush block copolymers, which demonstrates the importance of molecular shape in polymer self-assembly and extends the versatility of bottlebrush macromolecules as precursors to new nanomaterials.

The PS–PLA block copolymer (Scheme 1) was synthesized by our previously developed methodology that utilizes a combination of controlled radical and ring-opening polymerizations (Scheme S1, Supporting Information).¹⁷ First, a nearly symmetrical well-defined backbone was prepared by sequential reversible

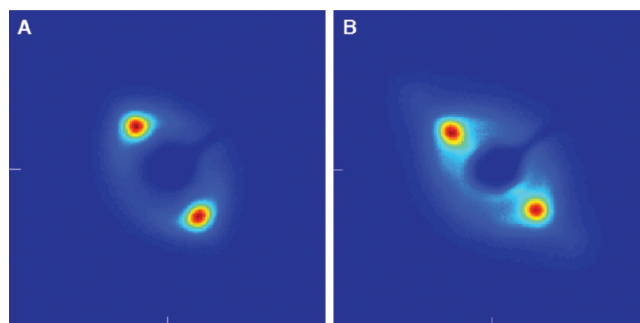


Figure 2. 2D SAXS patterns for aligned PS–PLA bottlebrush copolymer monoliths before (A) and after (B) PLA removal. The data are plotted as a function of q , with each edge representing $\pm 0.3 \text{ nm}^{-1}$ from center.

addition–fragmentation chain transfer (RAFT)¹⁸ polymerization of solketal methacrylate and 2-(bromoisobutryl)ethyl methacrylate (BIEM). Polystyrene branches of 4.8 kg/mol were grafted by atom transfer radical polymerization (ATRP)¹⁹ from the initiation sites of BIEM along the copolymer backbone. Subsequently, the ketal groups of poly(SM) backbone were removed to expose the diol groups, which served as initiators for the polymerization of D,L-lactide. Polylactide branches of 1.0 kg/mol were grafted by DBU catalyzed ring-opening polymerization.²⁰ Size exclusion chromatography (SEC) analysis of the final bottlebrush copolymer revealed a $M_n = 187.3 \text{ kg/mol}$ (relative to polystyrene standards) and a relatively low polydispersity index of 1.29 (Figure S1, Supporting Information). The absolute M_n of the bottlebrush block copolymer was calculated to be 1140 kg/mol by NMR analysis.¹⁷ The large discrepancy between the absolute and relative (SEC) molecular weights can be attributed to the highly branched polymer architecture. The final volume fraction of PLA was found to be 0.3 by NMR analysis.

Small-angle X-ray scattering (SAXS) analysis of melt-pressed and annealed (180°C) block copolymer samples revealed a strong primary scattering peak at $q = 0.09 \text{ nm}^{-1}$, corresponding to a d spacing of 70 nm (Figure S2, Supporting Information). A broad higher order reflection could also be observed centered at $q = \sqrt{7}q^*$, which is normally indicative of a hexagonal symmetry, but the broadness of the peak and the absence of other higher order reflections prevented an unambiguous identification of the morphology. In fact, the broad peak at higher q has some similarities with structure factor scattering of randomly distributed spheres or cylinders.²¹ After the self-assembled polymer melt was processed in a channel die at 180°C , which has been an effective tool for aligning cylindrical block copolymer morphologies in particular,²² the SAXS analysis indeed showed the presence of a highly oriented morphology aligned in the direction of flow (Figure 2a), with second-order orientation factor F_2 calculated to be 0.75.^{22–24} The high degree of alignment observed after channel die processing precludes the existence of a spherical morphology, given the linear spot pattern produced. Transmission electron microscopy (TEM) analysis of the asymmetric bottlebrush block copolymer revealed the formation of the cylindrical morphology (Figure 3). PLA cylinders appeared to be randomly distributed in the PS matrix, consistent with the absence of higher order reflections in SAXS. The average diameter of the cylinders was measured to be $47 \pm 8 \text{ nm}$ from the obtained TEM images.²⁵

The degradation of PLA was carried out under alkaline conditions, as reported previously.²² PLA removal from the aligned

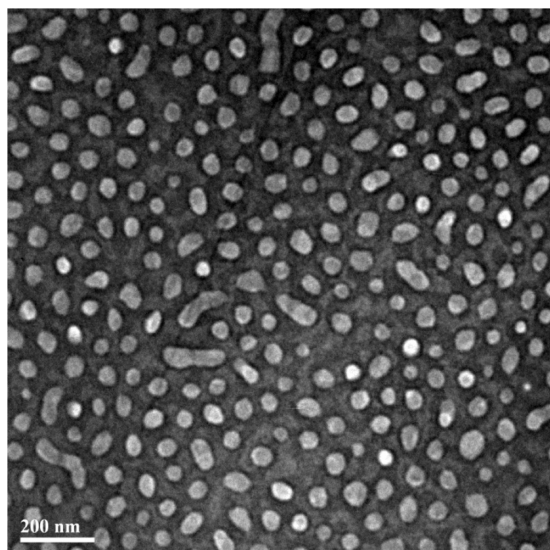


Figure 3. TEM image of the PS-PLA bottlebrush block copolymer (stained with RuO_4).

block copolymer monoliths was followed by ^1H NMR spectroscopy, where the signal at 5.2 ppm, corresponding to the methine protons of PLA, completely disappeared after degradation (Figure S3, Supporting Information). Additionally, in the FTIR spectrum, a strong PLA carbonyl peak at 1755 cm^{-1} disappeared after degradation, while a small peak at 1732 cm^{-1} remained (Figure S4, Supporting Information). The latter can be attributed to the carbonyl groups of the methacrylate backbone, which should remain intact after PLA degradation. The complete removal of PLA from macroscopic monolith samples (5 mm long) indicates the continuity of PLA domains throughout the sample. In the SAXS pattern obtained after PLA degradation (Figure 2b and Figure S2, Supporting Information), the position of the primary scattering peak and the degree of alignment ($F_2 = 0.72$) were in close agreement with values obtained from the precursor monolith, indicating that the morphology was preserved with high fidelity during the PLA degradation process.

Polymer monoliths fractured parallel and perpendicular to the direction of alignment were analyzed by scanning electron microscopy (SEM), which provided clear evidence for the formation of a porous structure. The images of samples fractured parallel to the direction of alignment show nanosize channels running through the sample (Figure S5, Supporting Information), while those fractured perpendicular to the alignment direction display a collection of closely packed nanopores (Figure 4 and Figure S6 in the Supporting Information). The pores do not seem to exhibit any hexagonal packing order, which would explain the lack of higher order reflections in SAXS and is consistent with TEM images obtained for the block copolymer before PLA degradation (vide supra). On the other hand, the pores exhibited a relatively narrow size distribution expected from the block copolymer self-assembly. The average pore diameter was measured to be $55 \pm 16\text{ nm}$ from the SEM images,²⁵ which is significantly larger than what is typically obtained from linear block copolymer precursors. This pore size does not represent the upper limit of what could be attained but demonstrates a feasibility of the utilized approach.

Another important outcome of the two-dimensional nature of the bottlebrush architecture is the presence of an undegraded

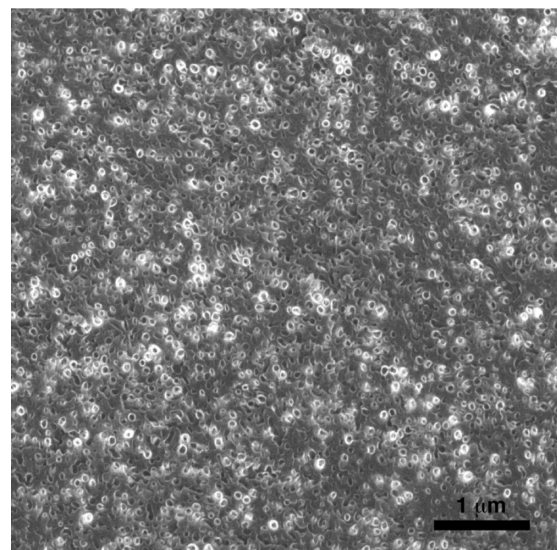


Figure 4. Scanning electron micrograph of a nanoporous material prepared from an asymmetric PS-PLA bottlebrush block copolymer.

backbone inside the pores that could serve for further functionalization. When PLA side chains are removed by acidic hydrolysis from the polymer monoliths, the polymethacrylate backbone that they were attached to remains inside the pores. Thus, after complete degradation, one should obtain a nanoporous polystyrene monolith with a hydrophilic, poly(methacrylic acid) coating on the inside (which comprises about 7% of the cylindrical domain). The presence of the residual carbonyl groups can be evidenced by FTIR analysis (Figure S4, Supporting Information), where a small peak at 1732 cm^{-1} is clearly distinguishable even after the complete removal of PLA. This carbonyl group vibration can be attributed not only to the hydrolyzed polymethacrylate backbone of the PLA brush but also to the backbone that is holding the PS brushes together. The ultimate proof for the existence of the hydrophilic coating inside the nanopores is their ability to uptake water. It has been demonstrated that nanoporous polystyrene monoliths prepared from linear PS-PLA precursors do not uptake water due to the fact that water cannot wet the interior surface of the hydrophobic polystyrene pores.²⁶ One has to utilize clever design strategies to overcome this problem, such as the use of triblock copolymer precursors.²⁷ On the other hand, monoliths prepared in this work from PS-PLA bottlebrush diblock copolymers appear to uptake water from a completely dry state, as evidenced by their slow sinking in deionized water (the density of polystyrene is higher than that of water at room temperature).

Direct analysis of water confined inside the nanopores was carried out by differential scanning calorimetry. Water-soaked nanoporous monoliths were cooled down to $-50\text{ }^\circ\text{C}$, allowing water to crystallize inside and outside of the pores. Subsequently, upon slow heating, one can observe two endotherms: one at $0\text{ }^\circ\text{C}$, corresponding to bulk ice, and the other at $-3\text{ }^\circ\text{C}$, corresponding to melting of nanocrystalline ice confined inside the pores (Figure 5). Using a standard thermoporometry analysis,²⁸ relying on the Gibbs–Thompson effect, one can estimate the expected melting point depression to be $-1\text{ }^\circ\text{C}$, based on the diameter of nanochannels. However, as others have demonstrated,^{29,30} melting point depression strongly depends on the interaction between the liquid and the pore wall surfaces, in this

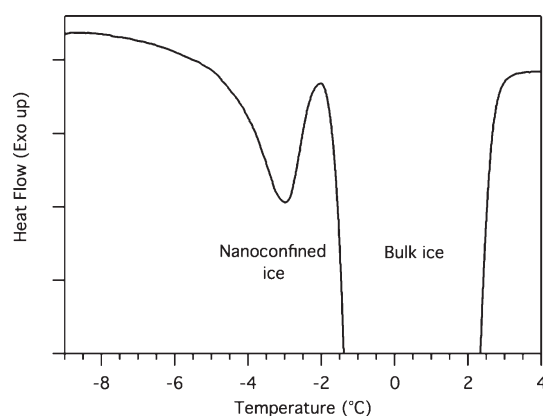


Figure 5. DSC analysis of water-filled nanoporous monoliths. The data were obtained on heating at 1 °C/min, after the sample was cooled down to −50 °C.

case coated with poly(methacrylic acid), which can explain the discrepancy between the calculated and experimentally observed values.

In summary, we have demonstrated that a PS-PLA bottlebrush block copolymer with asymmetric side chains can produce a cylindrical morphology upon melt self-assembly. This is the first example of a nonlamellae morphology obtained from a bottlebrush block copolymer, which highlights the important role that molecular shape plays in the self-assembly process. The cylindrical morphology was aligned under macroscopic shear, and PLA cylinders were selectively removed by alkaline hydrolysis, producing nanoporous monoliths with an average pore diameter of 55 nm. Such pore sizes are notably larger than what could be attained from linear diblock copolymer precursors. The remaining backbone inside the pores served as a functional coating rendering the nanopores hydrophilic, as demonstrated by the efficient water uptake. The described method expands the range of available pore sizes for nanoporous materials prepared from block copolymers, which will significantly broaden their utility for ultrafiltration and templating applications.

■ ASSOCIATED CONTENT

Supporting Information. Experimental details, Scheme S1, and Figures S1–S6. This material is available free of charge via the Internet at <http://pubs.acs.org>.

■ AUTHOR INFORMATION

Corresponding Author

*Email: jrzayev@buffalo.edu.

■ ACKNOWLEDGMENT

The financial support for this work was provided by the National Science Foundation (DMR-0846584). We also would like to thank Dr. Peter Bush for the help with SEM analysis.

■ REFERENCES

- (1) Bates, F. S.; Fredrickson, G. H. *Phys. Today* **1999**, *52* (2), 32.
- (2) Abetz, V. *Block copolymers*; Springer: Berlin and London, 2005.
- (3) Hillmyer, M. Nanoporous Materials from Block Copolymer Precursors. In *Block Copolymers II*; Abetz, V., Ed.; Springer: Berlin/Heidelberg, 2005; Vol. 190.

- (4) Jackson, E. A.; Hillmyer, M. A. *ACS Nano* **2010**, *4* (7), 3548.
- (5) Phillip, W. A.; O'Neill, B.; Rodwogin, M.; Hillmyer, M. A.; Cussler, E. L. *ACS Appl. Mater. Interfaces* **2010**, *2* (3), 847.
- (6) Ha, J.-M.; Wolf, J. H.; Hillmyer, M. A.; Ward, M. D. *J. Am. Chem. Soc.* **2004**, *126* (11), 3382.
- (7) Bang, J.; Jeong, U.; Ryu, D. Y.; Russell, T. P.; Hawker, C. J. *Adv. Mater.* **2009**, *21* (47), 4769.
- (8) Thurn-Albrecht, T.; Schotter, J.; Kastle, C. A.; Emley, N.; Shibauchi, T.; Krusin-Elbaum, L.; Guarini, K.; Black, C. T.; Tuominen, M. T.; Russell, T. P. *Science* **2000**, *290* (5499), 2126.
- (9) For exceptions to this rule, see: Xu, T.; Kim, H. C.; DeRouchey, J.; Seney, C.; Levesque, C.; Martin, P.; Stafford, C. M.; Russell, T. P. *Polymer* **2001**, *42* (21), 9091.
- (10) Sheiko, S. S.; Sumerlin, B. S.; Matyjaszewski, K. *Prog. Polym. Sci.* **2008**, *33* (7), 759.
- (11) Zhang, M. F.; Muller, A. H. E. *J. Polym. Sci., Polym. Chem.* **2005**, *43* (16), 3461.
- (12) Byun, M.; Bowden, N. B.; Lin, Z. Q. *Nano Lett.* **2010**, *10* (8), 3111.
- (13) Byun, M.; Han, W.; Qiu, F.; Bowden, N. B.; Lin, Z. Q. *Small* **2010**, *6* (20), 2250.
- (14) Zhao, L.; Goodman, M. D.; Bowden, N. B.; Lin, Z. Q. *Soft Matter* **2009**, *5* (23), 4698.
- (15) Zhao, L.; Byun, M.; Rzaev, J.; Lin, Z. Q. *Macromolecules* **2009**, *42* (22), 9027.
- (16) Xia, Y.; Olsen, B. D.; Kornfield, J. A.; Grubbs, R. H. *J. Am. Chem. Soc.* **2009**, *131* (51), 18525.
- (17) Rzaev, J. *Macromolecules* **2009**, *42* (6), 2135.
- (18) Moad, G.; Rizzardo, E.; Thang, S. H. *Aust. J. Chem.* **2005**, *58* (6), 379.
- (19) Matyjaszewski, K.; Xia, J. H. *Chem. Rev.* **2001**, *101* (9), 2921.
- (20) Lohmeijer, B. G. G.; Pratt, R. C.; Leibfarth, F.; Logan, J. W.; Long, D. A.; Dove, A. P.; Nederberg, F.; Choi, J.; Wade, C.; Waymouth, R. M.; Hedrick, J. L. *Macromolecules* **2006**, *39* (25), 8574.
- (21) Higgins, J. S.; Benoit, H. C. *Polymers and Neutron Scattering*; Oxford University Press: New York, 1997.
- (22) Zalusky, A. S.; Olayo-Valles, R.; Wolf, J. H.; Hillmyer, M. A. *J. Am. Chem. Soc.* **2002**, *124* (43), 12761.
- (23) de Gennes, P. G.; Prost, J. *The Physics of Liquid Crystals*; Oxford University Press: New York, 1993.
- (24) Sakurai, S.; Aida, S.; Okamoto, S.; Ono, T.; Imaizumi, K.; Nomura, S. *Macromolecules* **2001**, *34* (11), 3672.
- (25) The average diameter and the corresponding standard deviation were obtained from electron micrographs by analyzing more than 100 domains.
- (26) Rzaev, J.; Hillmyer, M. A. *Macromolecules* **2005**, *38* (1), 3.
- (27) Rzaev, J.; Hillmyer, M. A. *J. Am. Chem. Soc.* **2005**, *127* (38), 13373.
- (28) Brun, M.; Lallemand, A.; Quinson, J. F.; Eyraud, C. *Thermochim. Acta* **1977**, *21* (1), 59.
- (29) Ha, J. M.; Hillmyer, M. A.; Ward, M. D. *J. Phys. Chem. B* **2005**, *109* (4), 1392.
- (30) Rault, J.; Neffati, R.; Judeinstein, P. *Eur. Phys. J. B* **2003**, *36* (4), 627.